Full Paper: Bulk hyperbranched anionic polymerisation of glycidol initiated by methoxide anion has been studied at B3PW91/6-311+G(2d,p)//HF/6-31G/d′) and MP2/6-31+G(d′)//MP2/6-31+G(d′) levels of theory. The Isodensity Polarised Continuum model was applied to take into account the environment effect. The results of molecular modelling are in good agreement with experimental data. According to the calculations glycidol polymerisation is thermodynamically controlled. The attack on the unsubstituted glycidol end is thermodynamically preferred except for the very first polymerisation step. Fast proton exchange reaction takes place during the polymerisation giving rise to the branching reaction. While the linear growth is caused by primary alkoxide attack, the branching reaction occurs by secondary alkoxide attack on the next glycidol molecule. It was found that cyclisation reactions show higher activation energies and are less favourable thermodynamically compared to polymerisation.

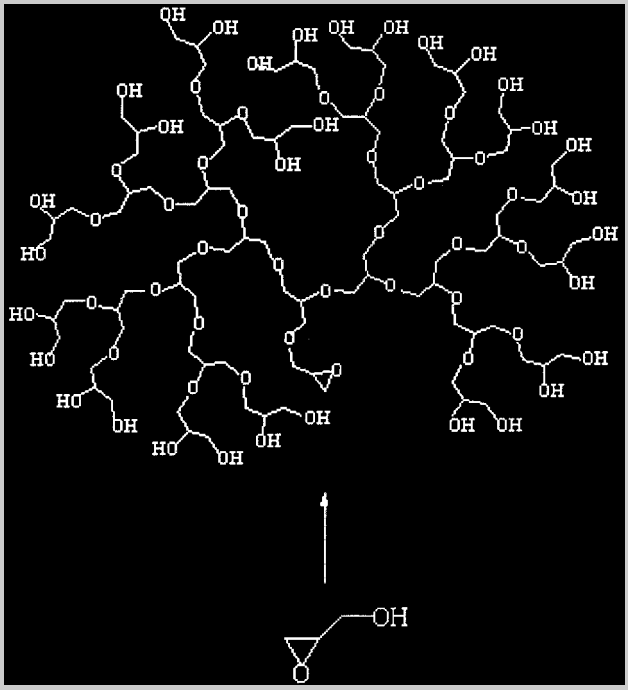

Hyperbranched polymerisation of glycidol.

Theoretical Study of Glycidol Hyperbranching Polymerisation

*Blanca Vazquez, Lioudmila Fomina, Raul Salazar, Serguei Fomine**

Instituto de Investigaciones en Materiales, Universidad Nacional Autónoma de México, Apartado Postal 70-360, CU, Coyoacán, México DF 04510, México
E-mail: fomine@servidor.unam.mx

Introduction

Recently, hyperbranched polymers have become of increasing interest as potential alternatives for the perfectly branched dendrimers that have to be constructed in a usually tedious, stepwise approach. On the other hand, hyperbranched polymers possess all the features of perfectly branched dendrimers and can easily be prepared by polycondensation reactions of AB_m monomers.[1] The main drawback of hyperbranched polymers obtained by the hyperbranched polymerisation of AB_m monomers is a broad molecular weight distribution combined with incomplete branching.

Another promising approach to hyperbranched polymers mentioned only in a few literature sources is the ring-opening polymerisation of cyclic latent AB_2 monomers.[2–4] This approach has successfully been used to synthesise various types of hyperbranched polyethers by the polymerisation of glycidol, a commercially available, highly reactive latent AB_2 monomer. The polymerisation of glycidol results in hyperbranched polyether with numerous hydroxyl end groups (Scheme 1). The first polymerisation of glycidol was described by Sandler and Berg[5] who considered branching as an undesired side reaction. Recently, Frey et al. have shown[2–4] that glycidol can be polymerised anionically to a hyperbranched polyether with a narrow molecular weight distribution and controlled molecular weight. Hyperbranched polyglycidol can be selectively modified using the chemical difference between the remaining linear glycerol hydroxyl units and peripheral vicinal hydroxyl groups[3] to produce a variety of hyperbranched polymers. A detailed analysis of polygycidol structure have been carried out[2]

  1022-1344/2001/0810–0762$17.50+.50/0

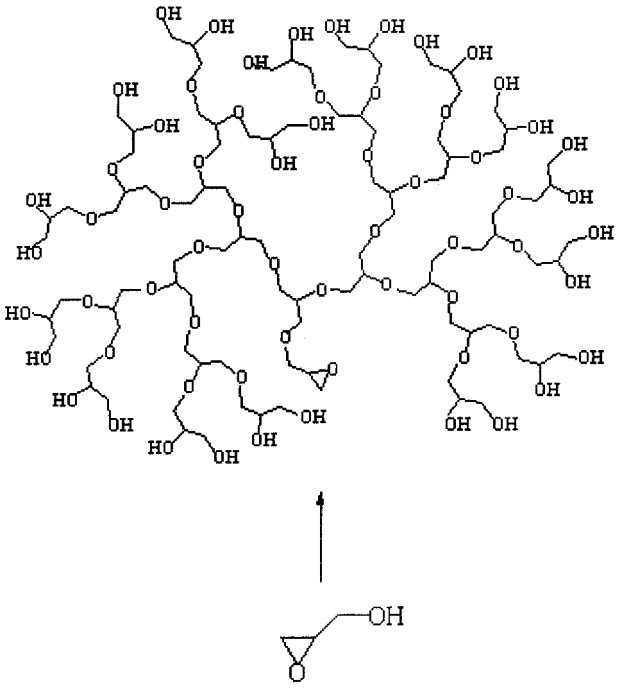

Scheme 1. Hyperbranched polymerisation of glycidol.

using NMR spectroscopy and matrix-assisted laser desorption/ionisation time-of-flight (MALDO-TOF) spectrometry. The aim of this contribution is to apply quantum chemistry tools for the analysis of hyperbranched polymerisation of glycidol and to compare the molecular modelling results with the experimental observations. Bulk anionic polymerisation of glycidol initiated by MeO^- was chosen as a model.

Computational Details

Due to the flexibility of the molecules studied, the conformational search was performed first to locate a global minimum for each molecule. A systematic algorithm using MMFF94 force field implemented in Titan program (Wavefunction, Inc., Schrodinger, Inc.) was used for the search of conformational space. The found conformations corresponding to global minima were used as input geometries for Gaussian 98 A9 revision programme.[6] Since the transition-state geometries are more demanding of the level of theory than equilibrium-state ones, first different methods were tested for the transition-state optimisation of a model reaction: the addition of hydroxyl anion to ethylene oxide. MP2/6-311+G(d,p)-level geometry was taken as a reference. Among different levels of theory tested such as HF/6-31+G, HF/6-31+G(d), HF/6-31+G(d′), HF/6-31G(d′), B3PW91/6-311+G(d,p) and B3LYP/6-311+G(d,p), HF/6-31G(d′) model reproduced the best MP2/6-311+G(d,p) geometry and, therefore, was chosen for all geometry optimisation. In some cases, the MP2/6-31+G(d′) level using the frozen core approximation was applied along with the HF/6-31G(d′) model. In all cases frequency jobs were run to ensure that either a minimum (zero imaginary frequencies) or a transition state (one imaginary frequency) is located. Zero-point energies calculated from frequency jobs were scaled by a factor of 0.91844[7] for HF/6-31G(d′) model to correct the total energies. To improve the total energies single-point energy calculations were run using Becke's three-parameter hybrid functional[8] the with Perdew–Wang91 correlation functional[9] using the 6-311+G(2d,p) basis set at HF/6-31G(d′)-optimised geometries. The activation energies for propagation steps were obtained as the difference between the total energy of a transition state and the total energy of corresponding van der Waals (VDW) complex formed by glycidol and an active species The initial geometry of these complex was obtained by running internal reaction coordination (IRC)[10] calculations starting from transition-state geometry at the HF/3-21G level, followed by the geometry optimisation of the VDW complex at HF/6-31G(d′) or MP2/6-31+G(d′) levels of theory. Before running IRC calculations the transition structure was optimized at the HF/3-21G level of theory followed by the frequency job to ensure that a single-order saddle point was found. The MaxPoint keyword was set to 25 together with IRC = REVERSE to reach the minimum only in one direction.

Solvation energies were calculated at the B3PW91/6-311+G(2d,p) level using the Isodensity Polarised Continuum Model.[11] It is difficult to estimate the dielectric constant of polymerising glycidol needed for solvation calculations, however, a reasonable guess can be made inspecting the dielectric constants of small molecules resembling structural units of polyglycidol. Thus, for glycerol, 1,3-propanediol, 1,2-propanediol, 1,2-ethanediol and ethylene oxide dielectric constants at 25 °C are 46, 35, 27, 35 and 13, respectively.[12] Therefore, a dielectric constant of 30 was used to model the solvation effect.

Results and Discussion

In the case of MeO^--initiated polymerisation of glycidol, the real initiating species is the anion formed by the proton abstraction from the glycidol hydroxyl group resulting from the fact that glycidol is much stronger acid than MeOH according to our calculations and the proton transfer reaction show lower activation energy (E_a) compared to E of propagation (Table 1). As glycidyl anion can attack either unsubstituted or substituted carbon, two different dimers **1.1** and **1.2** can be formed (Scheme 2). Each dimeric alkoxide can produce two trimers, having secondary or primary alkoxide. Another possibility is the intramolecular proton transfer to produce primary alkoxide **1.3** from secondary one **1.1**. Alkoxide **1.3** can further propagate to form trimers **2.3** and **2.4**. Primary alkoxide **1.2** can propagate in two different ways to give secondary and primary alkoxide trimers, **2.8** and **2.7**, respectively.

Table 1. Energies (ΔE) and activation (E_a) energies (kcal · mol^{-1}) of studied reactions.

Reaction	MP2[a]		B3PW91[b]			
	ΔE	E_a	ΔE	E_a	ΔE^{c}	E_a[c]
MeO^-+GLY = MeOH+GLY^-	−9.4	0.8	−26.9	−0.4	−22.8	0.0
GLY+GLY^- = 1.1	−45.7	5.3	−36.5	5.2	−17.6	13.9
GLY+GLY^- = 1.2	−41.7	7.4	−34.4	7.9	−22.9	5.9
1.1 = 1.3	3.7	5.3	2.9	−1.5	2.1	−4.8
1.1+GLY = 2.1	–	–	−29.2	11.0	−21.2	9.0
1.1+GLY = 2.2	–	–	−28.5	23.2	−18.5	14.1
1.3+GLY = 2.3	–	–	−34.5	11.6	−26.3	15.9
1.3+GLY = 2.4	–	–	−36.2	9.4	−26.8	10.9
2.3 = 2.5	–	–	5.5	2.4	3.5	1.9
2.1 = 2.6	–	–	7.0	6.8	6.7	−1.2
1.2+GLY = 2.7	–	–	−29.4	10.9	−15.8	19.8
1.2+GLY = 2.8	–	–	−33.3	9.4	−12.9	10.5
2.8 = 2.9	–	–	3.5	3.0	−0.5	−0.2
2.4 = 2.10	–	–	3.1	−2.7	6.3	−2.4
2.1 = 2.12	–	–	2.6	−2.3	−4.8	−5.6
2.10+GLY = 2.11	–	–	−25.1	12.4	−27.3	19.2
2.12+GLY = 2.13	–	–	−28.7	13.7	−11.7	14.7
2.10+GLY = 2.14	–	–	−23.1	20.6	−19	28.3
2.12+GLY = 2.15	–	–	−28.7	18.0	−12.4	22.0
1.2 = Cycle-1	−10.1	18.8	−6.6	17.8	−4.7	18.0
1.1 = Cycle-2	−13.0	13.2	−11.1	11.4	−14.6	12.5
1.3 = Cycle-3	−11.9	16.4	−8.4	15.7	−15.6	17.8

[a] MP2/6-31+G(d′)/MP2/6-31+G(d′) level of theory.
[b] B3PW91/6-311+G(2d,p)/HF/6-31G(d′) level of theory.
[c] Energies corrected using Isodensity Polarized Continuum Model at B3PW91/6-311+G(2d,p)/HF/6-31G(d′) level of theory.

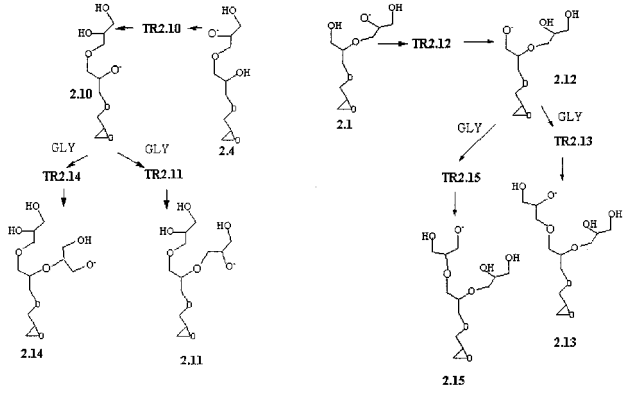

Scheme 2. Steps in glycidol polymerisation.

When intramolecular proton-transfer occurs in a trimer, then the alkoxides formed (Scheme 3) will produce branched structures (two of them for each trimer) giving four branched tetramers for trimers **2.10** and **2.12** as a models for branching formation during the polymerisation.

Since there is a glycidyl group at the beginning of each polymer chain, the cyclisation is of importance, especially at the early stages of growth when the formation of

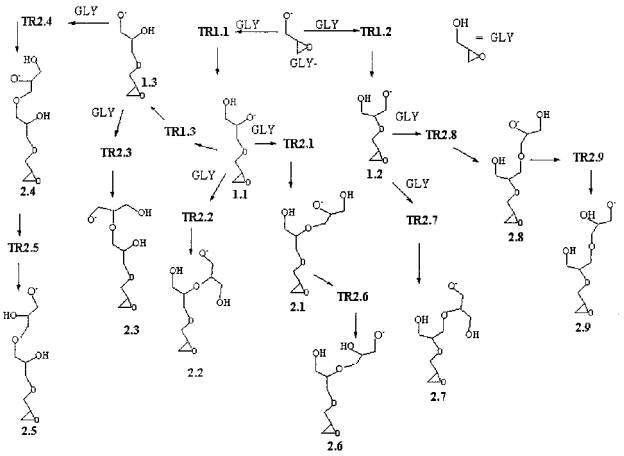

Scheme 3. Formation of branches during glycidol polymerisation.

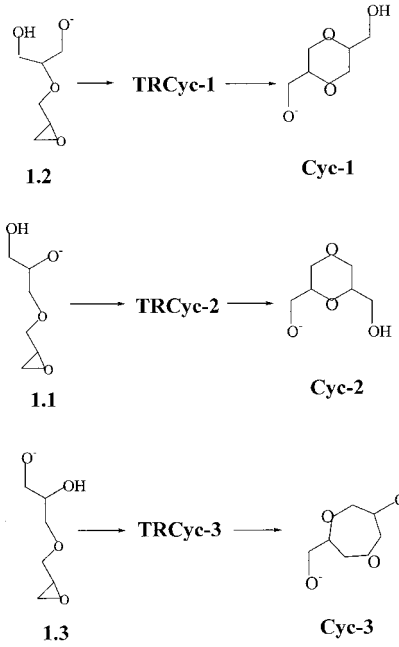

Scheme 4. Cyclisation reactions.

stable medium-sized cycles is possible. The formation of all possible medium-sized cycles (up to 7 members) is shown in Scheme 4. Table 1 listed the calculated reaction energies both, in gas phase and in solution while Tables 2, 3 and 4 show total and solvation energies of the studied molecules.

The anionic polymerisation of substituted oxiranes results in head-to-tail polymers[13–15] with the attack occurring at th eunsubstituted carbon of the oxirane ring. This is the case for the polymerisation of propylene oxide initiated with $Zn(OMe)_2$, styrene oxide polymerisation initiated with MeONa and aluminum triisipropanolate. Frey and coworkers[2] who studied the hyperbranched polymerisation of glycidol using partially deprotonated 1,1,1-tris(hydroxymethyl)propane as a polyfunctional

Table 2. Total energies (hartrees) including ZPE corrections and solvation energies (kcal · mol^{-1}) of the reaction intermediates participating in polymerisation of glycidol.

Molecules	Total energy		E_{solv}[c]
	MP2[a]	B3PW91[b]	
1.1	534.546232	−535.887653	−58.4
1.2	−534.539861	−535.884365	−65.8
1.3	−534.540279	−535.883060	−59.2
2.1	–	−804.144131	−56.5
2.2	–	−804.143014	−54.5
2.3	–	−804.147971	−57.1
2.4	–	−804.150686	−55.9
2.5	–	804.141885	−57.9
2.6	–	−804.132942	−56.8
2.7	–	−804.141119	−58.3
2.8	–	−804.147382	−51.5
2.9	–	−804.141884	−55.5
2.10	–	−804.145813	−52.7
2.11	–	−1072.39569	61.0
2.12	–	−804.140047	−63.9
2.13	–	−1072.395681	−53.1
2.14	–	−1072.392542	−53.9
2.15	–	−1072.395760	−53.8
Cycle-1	−534.555911	−535.894958	−63.9
Cycle-2	−534.566953	−535.905409	−61.9
Cycle-3	−534.559237	−535.896436	−66.4

[a] MP2/6-31+G(d′)/MP2/6-31+G(d′) level of theory.
[b] B3PW91/6-311+G(2d,p)/HF/6-31G(d′) level of theory.
[c] Solvation energies obtained with Isodensity Polarized Continuum Model at B3PW91/6-311+G(2d,p)/HF/6-31G(d′) level of theory.

initiator did not observe nucleophilic attack at the substituted end of the epoxide ring either.

The experimental enthalpy of oxirane polymerisation (−33.5 kcal · mol^{-1})[16] is in good agreement with energies for **1.1** and **1.2** intermediates formation (−36.6 and −34.5 kcal · mol^{-1}, respectively) in the gas phase at the B3PW91/6-311+G(2d,p)//HF/6-31G(d′) level of theory. The MP2/6-31+G(d′) model predicts the reaction energies to be more negative by several kcal · mol^{-1} for the first step of glycidol polymerisation (Table 1). Both models coincide in that the attack on the unsubstituted end is thermodynamically and kinetically favoured, in agreement with experimental observations for the ring-opening polymerisation of substituted oxiranes. The relatively low dielectric constant of oxirane (12.6) and of the respective derivatives substituted by nonpolar groups explains the good agreement of gas-phase calculation results for the formation of **1.1** and **1.2** intermediates with the experimental polymerisation enthalpy of oxirane and regioselectivity found in polymerisation of methyl and phenyl oxiranes. Moreover, for all trimers and tetramers the result of B3PW91/6-311+G(2d,p) calculations show lower activation energies and more negative reaction energies for the attack on unsubstituted end of glycidol. (Scheme 2 and 3).

Table 3. Total energies (hartrees) including ZPE corrections of located transition states and their respective solvatation energies (kcal · mol^{-1}).

Molecules	Total energy		E_{solv}[c]
	MP2[a]	B3PW91[b]	
TR1.1	−534.487404	−535.838186	−55.3
TR1.2	−534.487149	−535.834979	−57.1
TR1.3	−534.537732	−535.890135	−61.7
TR2.1	–	−804.090037	−55.5
TR2.2	–	−804.085563	−62.0
TR2.3	–	−804.089027	−49.6
TR2.4	–	−804.093225	−52.1
TR2.5	–	−804.146897	−56.4
TR2.6	–	−804.133224	−64.5
TR2.7	–	−804.078940	−58.5
TR2.8	–	−804.092291	−53.6
TR2.9	–	−804.142649	−54.7
TR2.10	–	−804.15498	−55.6
TR2.11	–	−1072.342401	−51.3
TR2.12	–	−804.147756	−59.8
TR2.13	–	−1072.335486	−51.8
TR2.14	–	−1072.333565	−54.8
TR2.15	–	−1072.333803	−48.5
TRCycle-1	−534.509890	−535.855997	−65.6
TRCycle-2	−534.525173	−535.869521	−57.3
TRCycle-3	−534.513757	−535.858031	−57.1

[a] MP2/6-31+G(d′)/MP2/6-31+G(d′) level of theory.
[b] B3PW91/6-311+G(2d,p)/HF/6-31G(d′) level of theory.
[c] Solvation energies obtained with Isodensity Polarized Continuum Model at B3PW91/6-311+G(2d,p)/HF/6-31G(d′) level of theory.

Table 4. Total energies (hartrees) including ZPE corrections of VDW-reaction complexes and their respective solvatation energies (kcal · mol^{-1}).

Complex	Total energy		E_{solv}[c]
	MP2[a]	B3PW91[b]	
C1.1	−534.495911	−535.846540	−64.0
C1.2	−534.498970	−535.847540	−55.0
C2.1	–	−804.107499	−53.5
C2.2	–	−804.122469	−53.0
C2.3	–	−804.107455	−53.9
C2.4	–	−804.108266	−53.6
C2.7	–	−804.096253	−67.4
C2.8	–	−804.107347	−54.7
C2.11	–	−1072.362145	−58.1
C2.13	–	−1072.357331	−52.8
C2.14	–	−1072.366460	−62.5
C2.15	–	−1072.362535	−52.5

[a] MP2/6-31+G(d′)/MP2/6-31+G(d′) level of theory.
[b] B3PW91/6-311+G(2d,p)/HF/6-31G(d′) level of theory.
[c] Solvation energies obtained with Isodensity Polarized Continuum Model at B3PW91/6-311+G(2d,p)/HF/6-31G(d′) level of theory.

Figure 1 shows the transition-state geometries for **1.1** and **1.2** molecules formation optimised at HF/6-31G(d′) and MP2/6-31+G(d′) levels of theory. MP2/6-31+G(d′) geometries can be considered as a reasonable standard to

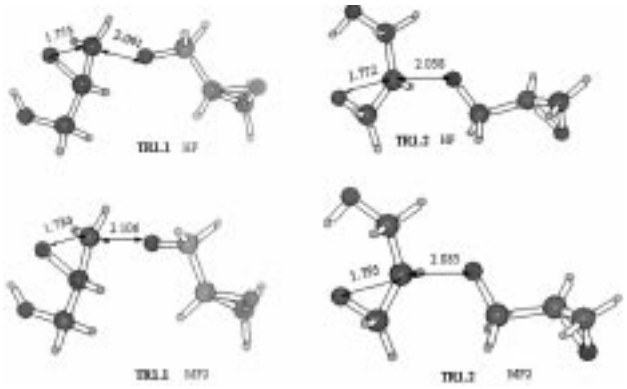

Figure 1. Transition-state geometries for the formation of **1.1** and **1.2** molecules optimised at HF/6-31G(d′) (HF) and MP2/6-31+G(d′) (MP2) levels of theory.

test HF/6-31G(d′)-optimised transition-state geometries. As can be seen, both geometries are quite similar. The difference in bond lengths is not exceeding 0.04 Å. Single-point energy calculations with a large basis set (6-311+G(2d,p)), using hybrid functional B3PW91, produce activation energies within 1.8 kcal · mol^{-1} of the MP2/6-31+G(d′)//MP2/6-31+G(d′) standard for propagation steps. Therefore the adopted model can be considered as adequate to study this type of system.

The situation is different when solvation is taken into account. In the first step, the addition of the glycidyl anion to glycidol, the attack on the substituted end of the oxirane ring is favoured thermodynamically and kinetically, in apparent contradiction to the experimental data.[2] Experimentally, no structures corresponding to an attack on the substituted end of the oxirane ring were found in polyglycidol. On the other hand, in all other modeled polymerisation steps, the product of an attack on an unsubstituted ring should be predominant, even when solvation is taken into account. Therefore, according to the calculations, the attack on the substituted end occurs only at initiation, and during the subsequent propagation, the attack is on the unsubstituted end. The difference for the initiation step is due to the larger dipole moment of **TR1.2** (3.5 D) compared to **TR1.1** (3.0 D) on the one hand, and the smaller dipole moment of **1.2** (5.6 D) compared to **1.1** (10.8 D), resulting in better solvation of **TR1.2** and **1.1** compared to **TR1.1** and **1.2**, respectively. A similar situation was observed experimentally during an aluminum triisopropanolate-initiated polymerisation of styrene oxide.[17] Although the polymerisation produced head-to-tail poly(styrene oxide), it was shown that the first addition gives a primary alcoholate active species and thus **1.2**-like product. According to the calculations, only the initiation step produces a primary alcoholate, adn this is followed by the attack on the usubstituted end of glycidol. Therefore, the concentration of **1.2**-type groups is very low in the polymer (one per macromolecule) and difficult to detect.

The effective branching process during the polymerisation of glycidol is closely related to a rapid inter- or intramolecular proton-exchange equilibrium leading to the deactivation of active sites after a few propagation steps. This implies the activation energy for the proton-transfer reaction to be lower than that of propagation step. Table 1 shows energies and E_a's for intramolecular proton transfer (Scheme 2 and 3). Even though the intermolecular proton-exchange reactions were not taken into account, there should not be much difference between intra- and intermolecular reaction from the energetic point of view. As seen from Table 1, the activation energies of proton transfer is always lower than these of the propagation step, thus explaining the effective branching observed during glycidol anionic polymerisation. When solvation is not taken into consideration, secondary alkoxides are found to be a few kcal · mol^{-1} more stable compared to primary ones, in agreement with the finding that in the gas-phase, tertiary alcohols are stronger acids than primary ones.[18] Solvation favours the stability of primary alkoxides and even more decreases the activation energy of proton exchange reaction. When comparing the activation energies for the attack of primary and secondary alkoxides on the next glycidol molecule (**1.1**–**2.1**, and **1.3**–**2.4**, Table 1) one can see that they are close to each other. Whereas in the gas-phase the primary alkoxide shows a slightly lower activation energy, the situation is reversed in solution. However the differences are too small to be meaningful (less than 2 kcal · mol^{-1} in both cases) for the theoretical model adopted. On the other hand, there is a clear thermodynamic preference for the product of primary alkoxide attack in all cases (Table 1, Scheme 2 and 3) explained by the less sterically hindered structure of the products of primary alkoxide attack. This result is in agreement with the experimental finding that the relative abundance of linear fragments formed by the attack of primary alkoxide is three times as much as those formed by the attack of secondary one,[2] suggesting that the polymerisation is a thermodynamically controlled reaction.

Cyclisation is one of the possible side reactions during glycidol polymerisation. For bulk polymerisation, which is the case of this study, cyclisation is less important when compared with solution polymerisation because cyclisation is a first-order reaction with respect to monomer concentration, whereas polymerisation is second-order. Two types of cyclisation reactions can be distinguished. The first one is the enthalpy-driven cyclisation taking place at the very beginning of the polymer chain growth to give six- and seven- membered rings (Scheme 4). The second one, not considered in this study, is the cyclisation occurring at later polymerisation stages and giving rise to macrocycle formation. In this case, entropy is of extreme importance, implying the necessity of frequency calculations for a number of very large

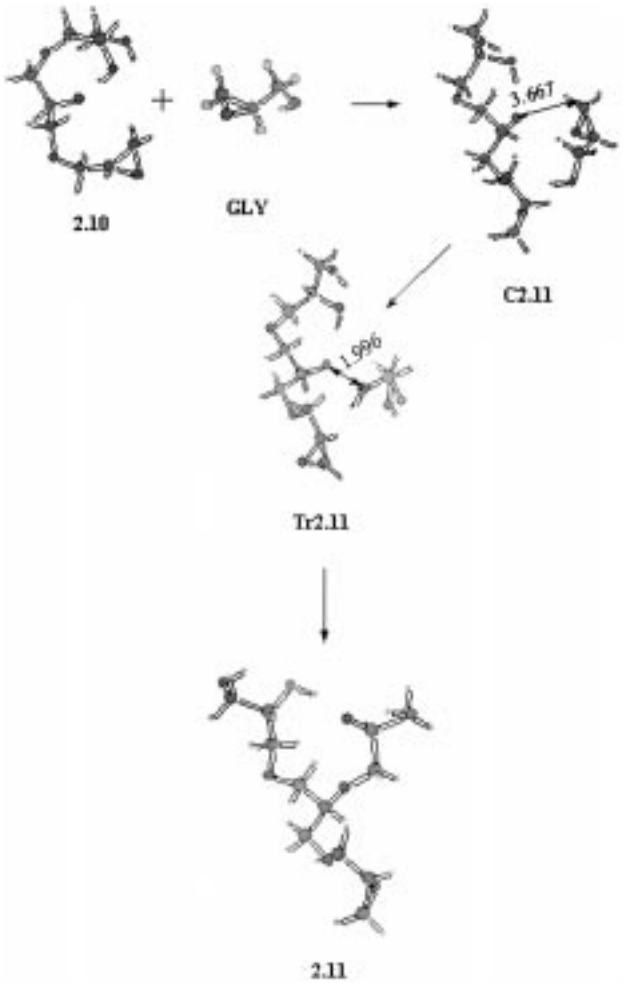

Figure 2. HF/6-31G(d′)-optimised geometries of intermediates participating in the formation of the branched structure **2.11**.

molecules at a good theoretical level, which is very computationally demanding.

Each dimer shown in Scheme 2 can produce the respective cycle. Intermediates **1.1** and **1.2** give six-membered cyclic species, while **1.3** produces seven-membered ring as a by-product of polymerisation. Every cycle is able to continue hyperbranched polymerisation similar to **1.1** or **1.2** species. Since it is the **1.2** dimer that should be predominant in the reaction mixture after initiation, it is only necessary to consider the formation of the **Cycle-1** molecule. Therefore, the **1.2** dimer can either react with another glycidol molecule to produce the **2.7** and **2.8** trimers, or to form cyclic **Cycle-1** species. As seen from the Table 1 the formation of the **2.8** trimer is more favourable kinetically and thermodynamically compared to cyclisation both in solution and in the gas phase. A similar situation holds for all other cyclic formation (**Cycle-2** and **Cycle-3**). The attack on another glycidol molecule rather than cyclisation is preferred both thermodynamically and kinetically. This is especially the case for bulk polymerisation where the monomer concentration is high. As a matter of fact, according to MALDI-TOF, no cycle formation was detected during the polymerisation of glycidol,[2] in agreement with calculations.

A comparison between linear and hyperbranched polymerisation can be made by inspecting reactions **1.1→2.1** and **2.10→2.11**, **1.1→2.2** and **2.10→2.14**, **1.3→2.3** and **2.12→2.15**, and **1.3→2.4** and **2.12→2.13** (Scheme 2 and 3 and Table 1). The first reaction of each pair represents the linear growth of the polymer chain while the second one is the corresponding branching reaction. As seen from the Table 1, in the gas phase, linear propagation is always thermodynamically favoured compared to hyperbranched propagation, due to steric hindrance. A similar situation holds (with one exception for **1.1→2.2** and **2.10→2.14** reactions) for activation energies, in which case a more crowded transition state results in higher activation energies for the formation of branched structures. The difference, however, is not as large as for reaction energies resulting from the "looser" structure of transition states compared to stable molecules When solvation is taken into account, the kinetic preference for forming a linear structure rather than a branched one becomes clearer than in the gas phase. On the other hand, the solvation reverses the energy difference between the linear and branched structures in the case of secondary alkoxide attack (**2.10→2.11**, Figure 2), making branching thermodynamically more favourable than linear growth. Therefore, in the case of linear growth, the product of primary alkoxide attack is thermodynamically preferred, while for the branching reaction, the attack of a secondary alkoxide produces a more stable product. This situation favours branching, because according to the modelling data, linear growth produces mainly secondary hydroxyl groups that cause an effective branching reaction. The theoretical work of Muller et al., based on a mechanistic model for AB_2 polymerisation assuming equal reactivities for A and B groups and neglecting solvation,[19] predicted that the degree of branching (DB) goes beyond the random polymerisation value of 0.5 only when glycidol is being added slowly to the initiator. It seems careful consideration of the solvation effect, the different reactivity of secondary and primary hydroxyl groups, and how the reactivity depends of the molecular size, is of importance to gain better insight into the mechanism of hyperbranching polymerisation of glycidol. According to our data, glycidol should produce a hyperbranched polymer with DB > 0.5 even in batch polymerisation processes.

Conclusions

Modern molecular modelling techniques allow us to describe the hyperbranched polymerisation of glycidol at a good theoretical level and to gain a better understanding of this process. The results of calculations agree well with experimental data, provided that thermodynamically

controlled polymerisation takes place. This suggestion is very reasonable taking into account the long reaction times (12 h) and high temperature (95 °C) of the polymerisation process.[2] The attack on the unsubstituted end of the oxirane ring is preferred in all steps except the very first where the **1.2** structure was found to be more stable and easy to form. All other things being equal, the primary alkoxide attack gives more stable products than the attack of secondary one in case of linear growth. On the other hand, the branching reaction produces a more stable product when attack of the secondary alkoxide occurs. The E_a's of proton transfer were found to be much lower than these of propagation, consistent with effective branching formation occurring during polymerisation. It seems that the formation of medium-sized rings is not an important side reaction.

Acknowledgment: This work was supported by grant 32560-E from CONACyT. We also appreciate financial support of the *Mexican Petroleum Institute*.

Received: March 1, 2001
Revised: June 15, 2001

[1] P. Flory, *Am. Chem. Soc*. **1952**, *74*, 2718.
[2] A. Sunder, R. Hanselmann, H. Frey, R. Mülhaupt *Macromolecules* **1999**, *32*, 4240.
[3] R. Haag, J. Stumbè, A. Sunder, H. Frey, A. Hebel, *Macromolecules* **2000**, *33*, 8158.
[4] A. Sunder, R. Mülhaupt, R. Haag, H. Frey, *Macromolecules* **2000**, *33*, 253.
[5] S. Sandler, F. Berg, *J. Polym. Sci., Polym. Chem. Ed.* **1966**, *4*, 1253.
[6] Gaussian 98, Revision A.9, M. J. Frisch, G. W. Trucks, H. B. Schlegel, G. E. Scuseria, M. A. Robb, J. R. Cheeseman, V. G. Zakrzewski, J. A. Montgomery, Jr., R. E. Stratmann, J. C. Burant, S. Dapprich, J. M. Millam, A. D. Daniels, K. N. Kudin, M. C. Strain, O. Farkas, J. Tomasi, V. Barone, M. Cossi, R. Cammi, B. Mennucci, C. Pomelli, C. Adamo, S. Clifford, J. Ochterski, G. A. Petersson, P. Y. Ayala, Q. Cui, K. Morokuma, D. K. Malick, A. D. Rabuck, K. Raghavachari, J. B. Foresman, J. Cioslowski, J. V. Ortiz, A. G. Baboul, B. B. Stefanov, G. Liu, A. Liashenko, P. Piskorz, I. Komaromi, R. Gomperts, R. L. Martin, D. J. Fox, T. Keith, M. A. Al-Laham, C. Y. Peng, A. Nanayakkara, M. Challacombe, P. M. W. Gill, B. Johnson, W. Chen, M. W. Wong, J. L. Andres, C. Gonzalez, M. Head-Gordon, E. S. Replogle, J. A. Pople, Gaussian, Inc., Pittsburgh, PA 1998.
[7] G. Petersson, T. Tensfeldt, J. A. Montgomery Jr., *J. Chem. Phys*. **1991**, *94*, 6091.
[8] A. Becke, *Phys. Rev. A* **1988**, *38*, 3098.
[9] J. Perdew, K. Burke, Y. Wang, *Phys Rev. B* **1996**, *54*, 16533.
[10] C. Gonzalez, H. B. Schlegel, *J. Phys. Chem*. **1990**, *94*, 5523.
[11] J. Foresman, T. Keith, K. Wiberg, J. Snoonian, M. Frisch *J. Phys. Chem*. **1996**, *100*, 16098.
[12] D. R. Lide, Ed., "*CRC Handbook of Chemistry and Physics*", 78th Edition, CRS Press, New York 1997–1998.
[13] S. Inoue, I. Tsukuma, M. Kawaguchi, T. Tsuruta, *Makromol. Chem.* **1967**, *103*, 151.
[14] Z. Jedlinski, J. Kasperczyk, A. Dworak, B. Matuszewska, *Makromol. Chem.* **1982**, *183*, 587.
[15] M. Sepulchre, A. Kassamaly, M. Moreau, N. Spassky, *Makromol. Chem*. **1988**, *189*, 2485.
[16] V. Ostrovskii, V. Khodzhemirov, V. Barkova, *Dokl. Akad. Nauk SSSR* **1970**, *191*, 1095; *Chem. Abstr.* **1970**, *73*, 35921.
[17] Z. Jedlinski, J. Kasperczyk, A. Dworak, *Eur. Polym. J.* **1983**, *19*, 899.
[18] R. Yamdagni, P. Kebarle, *J. Am Chem. Soc*, **1973**, *95*, 3504.
[19] W. Radke, G. Litvinenko, A. Muller, *Macromolecules* **1998**, *31* 239.